Journal of Applied Electrochemistry **34**: 591–599, 2004.

Corrosion mitigation of mild steel by new rare earth cinnamate compounds

F. BLIN[1,3,*], S.G. LEARY[2,3], K. WILSON[1,3], G.B. DEACON[2,3], P.C. JUNK[2,3] and M. FORSYTH[1,3]
[1]*School of Physics and Materials Engineering, Monash University, Wellington Rd., Clayton 3800, Victoria, Australia*
[2]*School of Chemistry, Monash University, Wellington Rd., Clayton 3800, Victoria, Australia*
[3]*Centre for Green Chemistry, Monash University, Wellington Rd., Clayton 3800, Victoria, Australia*
*(*author for correspondence, e-mail: frederic.blin@spme.monash.edu.au)*

Received 20 May 2003; accepted in revised form 8 January 2004

Key words: cinnamates, corrosion inhibitors, mild steel, organic inhibitors, rare earth metal salts

Abstract

Corrosion rate measurements based on weight loss (i.e., mild steel immersed for seven days in 0.01 M NaCl) and linear polarization resistance (LPR) techniques have shown that even low concentrations (200 ppm) of cerium and lanthanum cinnamates are able to significantly inhibit corrosion. Of all the compounds investigated in this work Ce(4-methoxycinnamate)$_3 \cdot 2\ H_2O$ and La(4-methoxycinnamate)$_3 \cdot 2\ H_2O$ compounds exhibited the greatest inhibition and, in comparison with the component inhibitors, a synergy was clearly observed. The mechanism of corrosion inhibition was investigated using cyclic potentiodynamic polarization (CPP) measurements. The results suggest that La(4-nitrocinnamate)$_3 \cdot 2\ H_2O$ and Ce(4-methoxycinnamate)$_3 \cdot 2\ H_2O$ behave as mixed inhibitors and improve the resistance of steel against localized attack.

1. Introduction

Due to their high efficiency:cost ratio, Cr(VI) compounds have been widely applied as corrosion inhibitors for many metals and alloy systems in aqueous media [1]. However, the use of chromates has recently been restricted in many countries due to their high toxicity and consequent environmental hazards [2]. Efforts towards replacing chromates have focussed on the search for and development of effective alternative 'green' inhibitors [3].

So far alternatives such as non-toxic oxyanions (molybdates) [3], organic compounds (thioglycollates, phosphonates) [4], or mixtures of inorganics (phosphates, borates, silicates) and surfactants (sulphonates) [5] have been investigated. A different approach for the replacement of chromates as corrosion inhibitors involves using cathodic and mixed inhibitors. Lanthanide compounds, also called 'rare earth metals' (REM), have been proposed as alternative inorganic 'green' inhibitors [6, 7]. Current availability of individual lanthanides (plus Y and La) in a state of high purity, relatively low cost and low toxicity has stimulated research into potential new applications. The lanthanides are very electropositive and reactive metals with a strong tendency to react with hard bases (phosphates, carboxylates). Lanthanide ions have been reported to form insoluble hydroxides [8], which enable them to be used as cathodic inhibitors. The use of REM salts to mitigate corrosion of mild steel was first reported in a patent by Goldie and McCarroll [9]. The potential of lanthanide salts of cerium, lanthanum and yttrium as corrosion inhibitors was also investigated by Hinton et al. [6]. They showed that $CeCl_3$ was an effective corrosion inhibitor for AS 1020 mild steel in quiescent soft tap water open to air [10]. $CeCl_3$ was also reported to continue to inhibit the corrosion of mild steel over a period of several months in a recirculating water system [6]. Since Isaacs and Davenport's experiments apparently contradict the claim that cerium was a cathodic inhibitor [7], Lai and Hinton have concluded that cerium chloride acts as a mixed inhibitor for the corrosion protection of mild steel [11].

Alkali salts of organic carboxylic acids have also been reported to prevent corrosion in water treatment facilities [12]. Their inhibition efficiency was attributed to adsorption of the inhibitor molecules via the carboxylate group on the metal surface, thereby forming a protective layer [13]. Benzoate anions are currently in use in corrosion inhibitor formulations and Mercer showed that their inhibition performance can be improved by the introduction of various substituents [12]. Cinnamates (3-phenyl propenoate, Figure 1) perform much better than benzoates and this has been attributed to the presence of the carbon double bond separating the benzene ring from the carboxylate group [12]. Cinnamate and nitrocinnamate, together with acetate, were studied in neutral and slightly alkaline oxidizing environments having low chloride concentrations and showed a good inhibition efficiency [14]. A mechanism

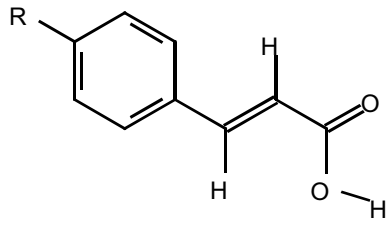

Fig. 1. Cinnamic acid (3-phenyl propenoic acid) structure (R=H).

of inhibition was proposed, in which insoluble stable iron carboxylate complexes were formed at the metal oxide surface with iron species maintained in the ferric state by dissolved oxygen.

A recent approach in designing 'green' inhibitors has been to investigate the attachment of an auxiliary effective organic inhibitor to the REM so as to utilize the corrosion inhibiting properties of both components of these new compounds in a potentially synergistic manner [15, 16]. To this end, compounds based on cinnamates attached to different lanthanide elements were investigated in this work. Weight loss and linear polarization measurements were used to determine the level of corrosion inhibition relative to a control and thus screen the inhibitor compounds. More detailed electrochemical studies, including cyclic potentiodyna mic polarization (CPP), were performed to investigate the primary corrosion inhibition mechanism of the most promising compounds.

2. Experimental details

2.1. *Materials*

The weight loss specimens (with dimensions 25 mm × 25 mm × 1 mm) were prepared from mild steel sheet AS1020 (Interlloy Pty, Victoria, Australia). The nominal composition of AS1020 is 0.18% C, 0.42% Mn, 0.009% P and 0.006% S.

Cylindrical working electrodes were machined from mild steel rod AS1020 (same supplier as above) to a diameter of 1 cm (surface area of 0.78 cm^2), encased in epoxy resin and attached to a Teflon coated holder to be used in the electrochemical measurements.

Reactions of REM trichlorides with stoichiometric amounts of the sodium salts of aromatic carboxylic acids resulted in high yielding REM tertiary carboxylates (cinnamates, substituted cinnamates) with very low water solubility (varying from 5×10^{-4} to 1.3×10^{-4} M). Carboxylic acids were initially dispersed in distilled water (50 mL) and treated with an equimolar amount of NaOH (0.5 M). The solution was adjusted to pH 7–8 by drop wise addition of dilute HCl. The sodium carboxylate solutions were slowly added to a stirred $LnX_3 \cdot x$-H_2O solution (Equation 1) whilst maintaining the pH below 6 by addition of dilute HCl. The precipitate was filtered and washed with ethanol followed by distilled water and dried in a vacuum desiccator for two days [17]. Details will be published elsewhere.

$$\mathrm{REM(X)_3 + 3\,NaL \xrightarrow{H_2O,pH<6} RE\,L_3 + 3\,NaX} \qquad (1)$$

where REM ≡ rare earth element, X ≡ Cl, NO_3. Purity of all compounds was determined by infrared spectroscopy, elemental analysis, metal analysis (acid digestions and EDTA titrations) and where possible X-ray powder diffraction.

All unsubstituted REM-cinnamates will be written in the format $REM(cin)_3$ (e.g., $La(cin)_3$, $Ce(cin)_3$) as they are anhydrous in nature. For simplicity the water of hydration is omitted in further discussion. Therefore $CeCl_3 \cdot xH_2O$ and $LaCl_3 \cdot xH_2O$ (where $7 \leqslant x \leqslant 9$) will be referred as $CeCl_3$, $LaCl_3$. The mixed hydrated REM-substituted cinnamates, $REM(4\text{-}OHcin)_3 \cdot 5\ H_2O$, $REM(4\text{-}MeOcin)_3 \cdot 2\ H_2O$ and $REM(4\text{-}NO_2cin)_3 \cdot 2\text{-}H_2O$ (where REM ≡ La and Ce) are shown as unsolvated below.

2.2. *Test solutions*

Distilled water and analytical grade reagent sodium chloride were used throughout the experiments. The test solutions were made by dissolving appropriate weights to make 50, 100, and when possible 200 ppm concentrations of REM(III) cinnamates (where REM ≡ La, Ce, Nd, Gd, Er, Y, Yb) in 0.01 M sodium chloride solution. Ethanol was added to solutions to help dissolution of the inhibitor in some cases; the ethanol was then evaporated from the solution prior to testing by heating the solution above the boiling temperature of ethanol for several hours. The solubility of the rare earth cinnamates was observed to increase slightly when dissolved in sodium chloride solutions. The sodium chloride concentration was chosen to allow sufficient degree of corrosion in a short period and yet still allow discrimination of inhibitor effectiveness. Less corrosion is expected with lower concentrations of NaCl (0.001 M) while extensive corrosion at higher concentrations (0.1 M) could lead to the exclusion of some potentially effective inhibitors.

All solutions were left open to air, exposed to a temperature-controlled laboratory atmosphere at approximately 22 °C and, once made, were left unstirred.

2.3. *Weight-loss measurements*

Weight loss measurements were performed initially to estimate relative corrosion rates in control and inhibition systems. Test specimens were abraded to 1200 grit, then rinsed with ethanol and air dried. Mild steel coupons were immersed in the solutions for a specific period of time (i.e., 7 d). Specimens were subsequently removed and cleaned in 30% orthophosphoric acid as per ASTM standard practices [18, 19].

The uncertainty in the determination of the corrosion rate for all the inhibitors and inhibitor compounds was evaluated to be less than 10% of the calculated value using the analytical equation given in the ASTM practices [18, 19]. This evaluated error was mainly due to the lack of precision in the determination of specimen dimensions. For each compound at a specific concentration two or more weight-loss measurements were conducted and in most cases gave fairly reproducible results (i.e. within the margin of expected experimental error).

2.4. *Potentiodynamic measurements*

The cell consisted of a 250 mL flask with a provision for a Luggin probe to be added through the base, and was used in conjunction with a Metrohm cap that allowed the working electrode and counter electrode (platinum wire) access to the solution. All potentials were measured with respect to a saturated calomel reference electrode (SCE). The working electrodes were prepared using silicon carbide paper to 1200 grit. They were rinsed in acetone and air dried before being immersed in the test solution. A computer-controlled Solartron SI 1280B potentiostat with CorrWare/CorrView software was used.

The potentiodynamic measurements were performed by immersing the working electrode in the test solution for 30 min to reach a reasonably steady and reproducible open circuit potential (OCP). Once a stable OCP was established, the measurement of the polarization resistance (R_p) was performed by scanning at a rate of 0.1667 mV s^{-1} within the range $E_{corr} \pm 10$ mV. Immersion for 24 h prior to measurements was undertaken to establish the time dependence of the inhibition process. These measurements were repeated twice and the standard deviation of R_p is reported.

Cyclic potentiodynamic polarization (CPP) measurements [20] were performed by scanning the potential from −0.6 V vs OCP to +0.6 V vs OCP (reverse) at a scan rate of 0.1667 mV s^{-1}. Repeat scan gave good reproducibility [20].

3. Results and discussion

3.1. *Weight-loss measurements*

Table 1 presents a summary of results obtained after immersing mild steel specimens for seven days in specified solutions. The corrosion rate (R) of inhibitor compounds at specific concentrations is displayed as μg m^{-2} s^{-1} and, mm y^{-1}. The percentage inhibition (η) is defined in Equation 2:

$$\eta = \frac{R(\text{control}) - R(\text{inhibitor})}{R(\text{control})} \times 100 \qquad (2)$$

Results on coupons immersed in 0.01 M NaCl and different concentrations of sodium dichromate ($Na_2Cr_2O_7$) are presented here to allow comparison. Among the different concentrations of sodium dichromate tested, the greatest inhibition was observed for $Na_2Cr_2O_7$ at 2000 ppm, displaying a corrosion rate of 4.4 μg m^{-2} s^{-1}.

For both $LaCl_3$ and $CeCl_3$ increasing the concentration of inhibitor beyond about 200 ppm led to an increased corrosion rate, possibly due to an increased [Cl^-] concentration [21].

From Figure 2, the REM(cin)$_3$ inhibitors (where REM ≡ Y, La, Ce, Nd, Gd, Er, Yb) at low concentration (50 ppm) appear to promote metal dissolution and display a corrosion rate close to or higher than that of the control. In almost all cases, the corrosion rates in the

Table 1. Calculated corrosion rates (μg m^{-2} s^{-1}, mm y^{-1}) and percentage inhibition (η) for mild steel coupons immersed in specific solutions for seven days. Uncertainty in corrosion rates is less than 10% of the values presented

Solutions	Concentration /ppm	Concentration /M	Corrosion rate /μg m^{-2} s^{-1}	Corrosion rate /mm y^{-1}	Inhibition, η /%
Control–NaCl	580	1.0×10^{-2}	34.7	0.139	0
$Na_2Cr_2O_7$	2000	7.3×10^{-3}	4.4	0.018	87
$LaCl_3$	217	5.5×10^{-4}	13.0	0.052	63
$CeCl_3$	200	5.1×10^{-4}	6.3	0.025	82
Na(cinnamate)	250	1.5×10^{-3}	6.3	0.025	82
Na(4-MeOcin)	250	1.0×10^{-3}	8.8	0.035	75
Na(4-NO_2cin)	250	1.2×10^{-3}	5.9	0.024	83
Na(4-OHcin)	250	1.3×10^{-3}	5.8	0.023	83
Y(cin)$_3$	162	3.0×10^{-4}	6.0	0.024	83
La(cin)$_3$	200	3.4×10^{-4}	6.0	0.024	83
La(4-OHcin)$_3$	500	7.0×10^{-4}	3.2	0.013	91
La(4-MeOcin)$_3$	191	2.7×10^{-4}	4.0	0.016	88
La(4-NO_2cin)$_3$	190	2.5×10^{-4}	2.8	0.011	92
Ce(cin)$_3$	180	3.1×10^{-4}	8.1	0.032	77
Ce(4-OHcin)$_3$	200	2.8×10^{-4}	5.7	0.022	84
Ce(4-MeOcin)$_3$	200	2.8×10^{-4}	4.5	0.018	87
Nd(cin)$_3$	150	2.6×10^{-4}	5.9	0.024	83
Gd(cin)$_3$	160	2.7×10^{-4}	5.0	0.020	86

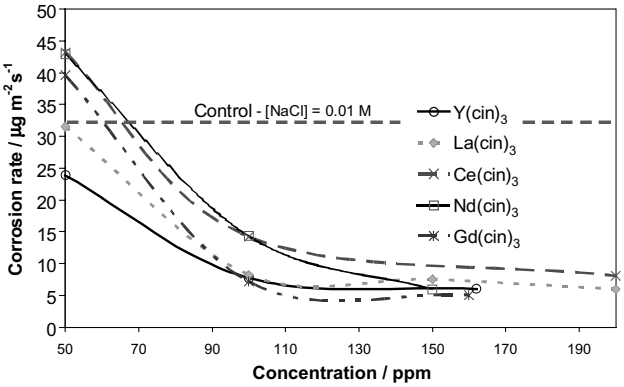

Fig. 2. Change in corrosion rate (μg m^{-2} s^{-1}) as a function of concentration (ppm) of different REM-cinnamate compounds. Mild steel coupons immersed for seven days in 0.01 M NaCl and specified inhibitors. Thick horizontal dotted line represents the average corrosion rate of the control. Uncertainty in corrosion rates is less than 10% of the values presented.

presence of REM(cin)$_3$ compounds were dramatically reduced as the concentration of inhibitor increased. Based on these results alone this behaviour is consistent with anodic inhibition [16].

Upon initial testing, La(cin)$_3$ at 100 ppm displayed the best inhibition and was therefore selected to be investigated using potentiodynamic techniques. However, some discrepancies were later observed, with several 7 day weight loss measurements having corrosion rates ranging from 1 to 12 μg m^{-2} s^{-1}. This scatter may be expected for an anodic inhibitor where, at times, its low concentration may not be sufficient to stifle the propagation of corrosion, which is initiated by chlorides' attack of the oxide film. On the other hand a synergy was clearly present in the case of La(cin)$_3$ at a concentration of 200 ppm, where this compound displayed an increased corrosion inhibition over its individual components at equivalent concentrations.

The inhibition performance of benzoate anions was previously reported to be improved with the introduction of –CH$_3$, –NO$_2$, –NH$_2$, –OH or –COOH groups [12] and even enhanced by having these substituents in the para position. Hence, rare earth para-substituted cinnamates (i.e., REM(4-OHcin)$_3$, REM(4-MeOcin)$_3$ and REM(4-NO$_2$cin)$_3$, where REM ≡ La and Ce) were investigated; the results are presented in Table 1. A comparison with the sodium salts is also given here.

Upon inspection, the mild steel coupons immersed for seven days in 250 ppm Na(4-OHcinnamate) and 250 ppm Na(4-NO$_2$cinnamate) did not show visible signs of corrosion and did not appear to leave any obvious film on the surface. The corrosion rates calculated from the weight loss data were generally found to be higher with the sodium salts than that of their rare earth substituted analogues. However, it must be remembered that these concentrations (250 ppm) were significantly lower than normally used for sodium carboxylates in optimum cases (above 2000 ppm) [22].

As shown in Table 1, all lanthanum para-substituted cinnamate compounds showed a marked improvement in terms of inhibition compared with La(cin)$_3$ (5.9 μg m^{-2} s^{-1}) at a concentration of 200 ppm. La(4-NO$_2$cin)$_3$ at a concentration of 190 ppm displayed the best inhibition of all compounds investigated in this work, giving a 7 day weight loss result of 2.8 μg m^{-2} s^{-1} and leaving the coupons pristine for the whole period of testing.

Like their lanthanum counterparts, Ce(4-OHcin)$_3$ and Ce(4-MeOcin)$_3$ showed a marked improvement over the unsubstituted Ce(cin)$_3$ compound at about the same concentration (200 ppm). The surface of the coupons immersed in 200 ppm Ce(4-MeOcin)$_3$ also appeared corrosion free.

Previous mechanistic studies carried out on sodium cinnamate and its derivatives on steel [12, 14] have proposed that an insoluble iron-carboxylate complex forms at the metal oxide surface, maintaining the underlying oxide in the ferric state by acting as a redox bridge to the oxidant in the aqueous medium. The coupons immersed in solutions containing La(cin)$_3$ or its substituted analogues were found to be covered with a uniform yellow, persistent film. Interestingly, no visible films were observed in the case of either La(4-NO$_2$cin)$_3$ or Ce(4-MeOcin)$_3$, even though these two compounds displayed the best corrosion inhibition. Further investigation of the surface of the coupons using ATR, SEM/EDXS is being carried out to correlate the results with the proposed inhibition model and will be presented elsewhere.

3.2. *Electrochemical measurements*

3.2.1. *Linear polarization resistance measurements*

By making several assumptions, the corrosion current density (i_{corr}) can be calculated from the Stern–Geary equation [23]. However, bearing in mind that the polarization resistance (R_p) as measured by LPR is inversely proportional to the corrosion current density, it is simpler to focus on the general trends and magnitude of the changes in R_p against a control sample. The percentage inhibition (η) calculated from the polarization resistance measurements as a function of time for different REM-cinnamate compounds is

Table 2. Polarization resistance, R_p (kΩ cm^2), and corrosion potential, E_{corr} (V vs SCE), values as calculated (R_p) from LPR measurements or extracted (E_{corr}) from potentiodynamic measurements. $\Delta E \pm 0.01$ V

Solution tested	R_p /kΩ cm^2		Inhibition, η /%		E_{corr} /V	
	30 min	*24 h*	*30 min*	*24 h*	*30 min*	*24 h*
Control – 0.01 M NaCl	2.1 ± 0.3	0.5 ± 0.1	0	0	−0.42	−0.45
250 ppm Na(cinnamate)	20 ± 2	2.2 ± 0.1	89	77	−0.22	−0.36
217 ppm $LaCl_3$	10.8 ± 0.4	6.3 ± 0.2	81	92	−0.62	−0.64
200 ppm $CeCl_3$	19.1 ± 0.3	25 ± 2	89	98	−0.59	−0.69
200 ppm $La(cin)_3$	3.7 ± 0.3	3.7 ± 0.1	45	86	−0.44	−0.51
180 ppm $Ce(cin)_3$	17 ± 2	14 ± 5	88	96	−0.17	−0.15
100 ppm $La(4\text{-}NO_2cin)_3$	18 ± 3	3.3 ± 0.1	88	85	−0.21	−0.45
190 ppm $La(4\text{-}NO_2cin)_3$	10 ± 1	9.5 ± 0.3	80	95	−0.21	−0.31
200 ppm $Ce(4\text{-}MeOcin)_3$	4 ± 2	23 ± 4	44	98	−0.31	−0.36

calculated according to Equation 3 and is presented in Table 2. R_p (ΔR_p being the standard deviation) was measured after the electrode was immersed for 30 min and 24 h in specified solutions. The corrosion potentials E_{corr} (vs SCE, $\Delta E \pm 0.01$ V) were extracted from the polarization curves.

$$\eta = \frac{(R_p(\text{inhibitor}) - R_p(\text{control}))}{R_p(\text{inhibitor})} \times 100 \qquad (3)$$

The polarization resistance obtained for 250 ppm Na(cinnamate) from LPR measurements was shown to decrease with time. This is consistent with Na(cinnamate) being reported to act primarily as an anodic inhibitor [22], where a decrease in concentration of the inhibitor led to an increase of the corrosion rate.

The percentage inhibition as calculated from LPR measurements in the case of the solutions $CeCl_3$ (200 ppm) and $LaCl_3$ (217 ppm) dramatically increased with time in solution. This is also consistent with previous studies [24], where inhibition of cathodic reactions was reported to occur at longer times.

Interestingly, both $La(cin)_3$ (200 ppm) and $Ce(cin)_3$ (180 ppm) behaved similarly to their chloride analogues, displaying an increased polarization resistance with time and, more significantly, this trend is further observed in the case of $Ce(4\text{-}MeOcin)_3$, which strongly suggests a significant contribution of the cathodic inhibition to the overall corrosion mitigation process. $La(4\text{-}NO_2cin)_3$ displayed a fairly constant R_p with time at a concentration of 190 ppm while at lower concentration (100 ppm) the high initial polarization resistance value was shown to decrease dramatically over time of exposure. The decreasing R_p at low concentration could be indicative of the anodic character of this inhibitor and suggests that as more corrosion sites are initiated with time, this low level of inhibitor compound is not sufficient to maintain good corrosion inhibition.

3.2.2. *Cyclic potentiodynamic polarization (CPP) measurements*

The mechanism of inhibition or acceleration may be better understood by investigating the electrochemical behaviour over a larger potential range. Typical polar-

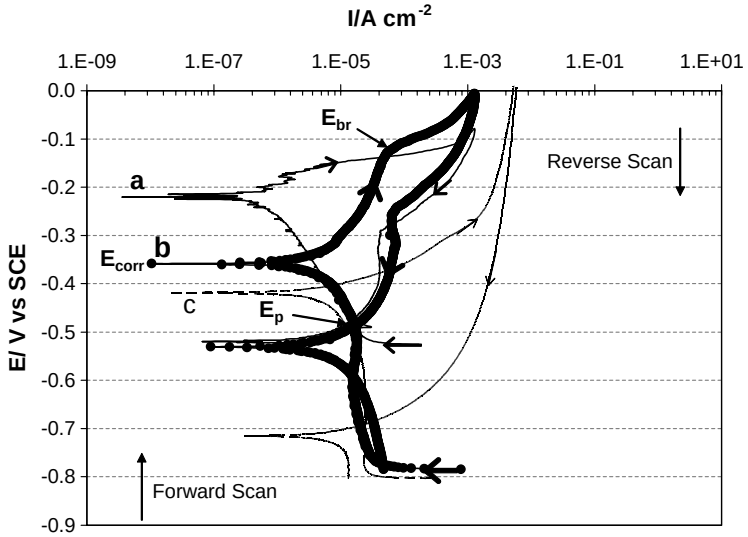

Fig. 3. Example of cyclic potentiodynamic polarization (CPP) scan. Mild steel electrode immersed for 30 min in 0.01 M NaCl solution and 250 ppm Na(cinnamate). Light scan (a) and dark scan (b) correspond, respectively, to the 30 min and 24 h immersion time in solution. The very light curve (c) is that of the control after 30 min in solution.

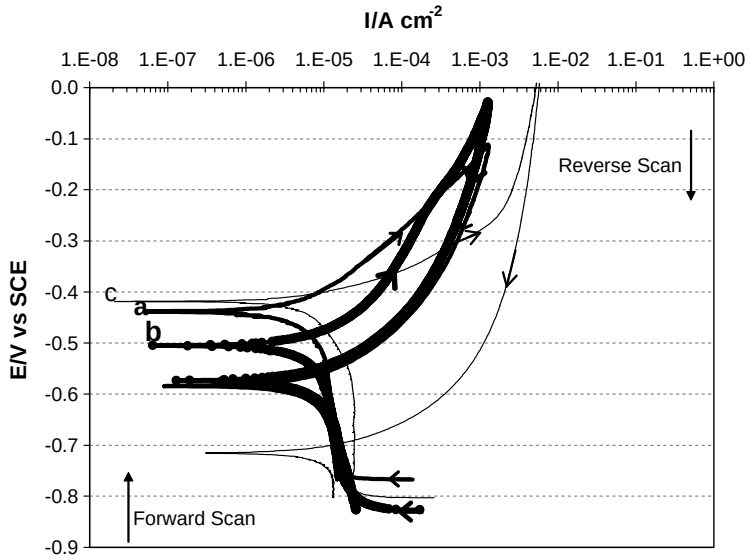

Fig. 4. CPP scans in 0.01 M NaCl and 200 ppm $La(cin)_3$. Key for (a), (b) and (c) as stated in Figure 3.

ization curves obtained for selected inhibitors are presented in Figures 3 to 7.

Figure 3 presents a typical CPP [20] scan obtained in this work for Na(cinnamate) for both 30 min and 24 h exposure. Data for a control experiment (i.e., the electrode immersed in 0.1 M NaCl) is included for comparison. This Figure indicates the definitions to be used in later discussion, pointing out E_{corr}, E_p and E_{br}, the corrosion potential, protection potential and breakdown (or pitting) potential, respectively. If the potential is pushed above a critical potential, called the breakdown potential, E_{br}, the current increases by orders of magnitude for small increases of potential (transpassive region). The more electropositive the E_{br} at a fixed scan rate, the less susceptible steel is to the initiation of localized attack [25]. The point of intersection of the forward and reverse scans is termed the protection potential, E_p. The potential of the steel must be above E_p for existing areas of localized corrosion to propagate. The more electropositive E_p, the less likely localized corrosion will continue to occur. The greater the difference between E_p and the breakdown potential, E_{br}, the greater the tendency for pitting corrosion [25]. In the case where a clear passive region is observed, E_{br} is well defined. However, in extreme conditions, where passivity is not visibly present this parameter cannot be clearly identified. The control curve after 30 min immersion is an example where passivity is not evident. This curve is included in all subsequent figures for comparison. In Figure 3 E_p cannot be considered as a real protection potential as defined above as it stands below the corrosion potential. This behaviour was observed in all scans presented here and may reflect more damage than can be repaired by these inhibitors under extreme conditions.

(a) *Electrochemical behaviour of mild steel in solutions of cinnamate and rare earth inhibitor.*

As expected from the literature [22], Na(cinnamate) containing solutions (Table 2 and Figure 3) displayed an initial E_{corr} value more anodic than the control and a

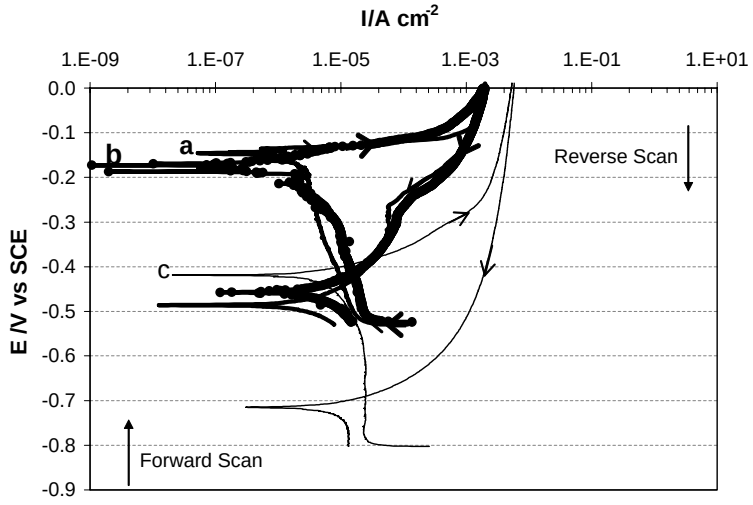

Fig. 5. CPP scans in 0.01 M NaCl and 180 ppm $Ce(cin)_3$. Key for (a), (b) and (c) as stated in Figure 3.

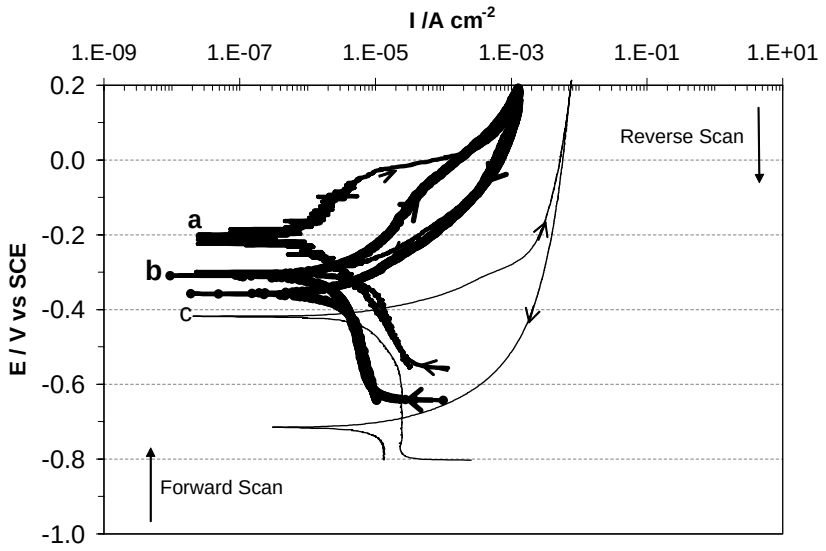

Fig. 6. CPP scans in 0.01 M NaCl and 190 ppm La(4-NO_2cin)$_3$. Key for (a), (b) and (c) as stated in Figure 3.

high initial polarization resistance. The hysteresis loop after 24 h (curve (b) in Figure 3) in solution was smaller than after 30 min, which suggests that the risk of localized corrosion is reduced even though not suppressed. The anodic arm was shifted towards greater current densities with time, which may explain the dramatic drop in R_p. However, after 24 h immersion the anodic arm displayed a pseudo-passive region (the anodic current was much lower than that of the control over the anodic region). This behaviour indicated that Na(cinnamate) acts primarily as an anodic inhibitor.

For the lanthanum chloride inhibited solutions (not displayed here) there was little difference when comparing the curves after 30 min and 24 h. E_{corr} was far more electronegative than that of the control, suggesting that $LaCl_3$ acts primarily as a cathodic inhibitor. The CPP scans obtained after immersing the electrode in 200 ppm $CeCl_3$ (not displayed here) solution gave an early E_{corr} more electronegative than that of the control, but E_{corr} shifted to more cathodic values with time. These observations were consistent with the literature, where $CeCl_3$ was also reported to act primarily as a cathodic inhibitor under these conditions [6].

(b) *Electrochemical behaviour of mild steel in solutions with REM-cinnamate compounds*

The corrosion potential of the steel in La(cin)$_3$ (200 ppm) after 30 min in solution (Table 2) shifted cathodically compared to that for steel in the control conditions. After 24 h, E_{corr} shifted towards even more negative values. This behaviour is likely to be linked to the further suppression of the cathodic reactions, for example by forming a barrier film that can block the electronic/ionic transport needed for the oxygen reduction reactions (assuming oxygen reduction is the dominant cathodic reaction under these conditions). Cathodic inhibition has previously been shown to

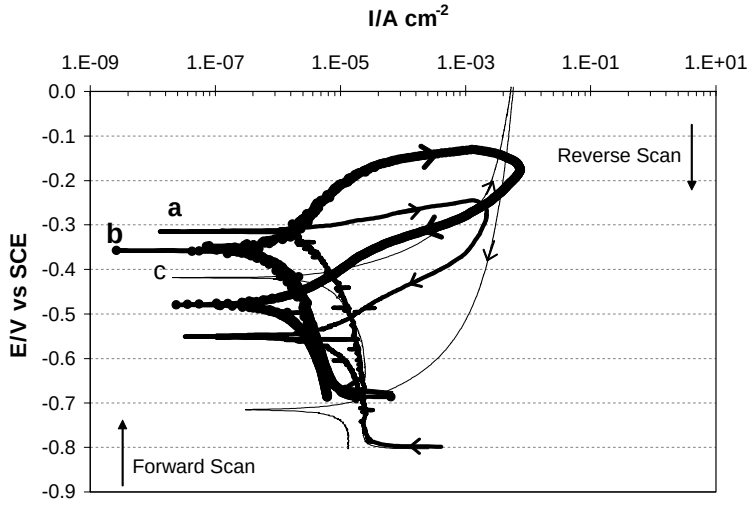

Fig. 7. CPP scans in 0.01 M NaCl and 200 ppm Ce(4-MeOcin)$_3$. Key for (a), (b) and (c) as stated in Figure 3.

require a longer time to take effect [24]. On the other hand $La(cin)_3$, shown in Figure 4, displayed an increased anodic slope with time and showed a 'pseudo-passive' region. The hysteresis loop was significantly diminished as compared with the control and even more so after 24 h. Traditionally the protection potential, E_p, would be greater than E_{corr}, as mentioned earlier. Nevertheless the inhibitor decreased the difference between E_p (as defined previously) and E_{corr}, which suggests that the likelihood of pitting propagation has been reduced. Given the shift of the anodic current towards lower current densities combined with the shift of E_{corr} to more negative values, it now appears that that $La(cin)_3$ behaves as a mixed inhibitor.

In the case of $Ce(cin)_3$ (Figure 5) at 180 ppm, E_{corr} was very electropositive (noble) compared to that of the control. There did not appear to be any major differences in terms of E_{corr} or hysteresis behaviour with time of exposure. In this case, at least over a 24 h period, it seemed that the anodic inhibition mechanism dominated. The polarization resistance (Table 2) was far greater than that of the control and appeared to have been unaffected by exposure time given the large standard deviation obtained for the 24 h immersion condition (± 5 kΩ cm^2). At this concentration, the early R_p value was, however, less than that of $CeCl_3$ or Na(cinnamate). This is probably due to the fact that the constituents of $Ce(cin)_3$ are not present at their individual 'optimum' concentrations. Therefore the effective inhibition of $Ce(cin)_3$ appeared superior to that of either components (at equivalent concentrations), confirming a synergistic response of the compound.

3.2.3. *Electrochemical behaviour of mild steel in solutions with para-substituted REM-cinnamate compounds*

The introduction of methoxy- and nitro-groups in the para position of the cinnamate was shown from weight-loss studies to give remarkably improved inhibition performance, especially by $La(4\text{-}NO_2cin)_3$ and $Ce(4\text{-}MeOcin)_3$ at a concentration of approximately 200 ppm. The CPP scans for these two compounds are given in Figures 6 and 7.

On the upward scan, after 30 min immersion in $La(4\text{-}NO_2cin)_3$, the anodic current density was suppressed by several orders of magnitude as compared with the control curve. Once the potential had been increased well into the pitting region, the reverse scan displayed an increased anodic current density (almost two orders of magnitude) thus leading to a large hysteresis loop. Nevertheless, in the reverse sweep the current density was still lower than the control. Thus this inhibitor was evidently behaving anodically under these conditions and for this concentration.

After 24 h immersion in solution, the electrode response in this case was significantly altered. The cathodic behaviour of the $La(4\text{-}NO_2cin)_3$ inhibition is now more evident. The current density in the cathodic arm of the forward scan was significantly depressed (compared with the 30 min immersion). Furthermore the E_{corr} value was also shifted towards more negative potentials. The anodic behaviour was less evident although still present; the forward scan displayed a significantly higher anodic current density while the reverse scan overlaps the shorter term measurement. This suggests that Cl^- induced pitting cannot be completely suppressed with relatively low inhibitor concentration. The combination of the results after both immersion times clearly suggests that this compound behaves as a mixed inhibitor. Once again it can be seen that the cathodic mechanism takes longer to become apparent.

In the case of electrodes immersed in $Ce(4\text{-}MeOcin)_3$ solutions (Figure 7) a dramatic effect on the CPP curves was observed suggesting significantly improved inhibition. This is consistent with the R_p data presented earlier. Initial E_{corr} was more anodic than the control but shifted towards more negative values with increased immersion times. In contrast to $Ce(cin)_3$, the $Ce(4\text{-}MeOcin)_3$ inhibitor showed evidence of a pseudo passive region between approximately -0.2 and -0.3 V. No such region was observed for the unsubstituted cinnamate compound. Thus it appears that the para substitution enhanced the anodic contribution to inhibition. At longer times the cathodic arm shifted towards lower current densities. Again these results strongly suggest a mixed inhibition behaviour.

4. Conclusions

The combination of cinnamate (and substituted cinnamate) compounds and cerium and lanthanum have been shown to have excellent inhibition performance for mild steel in 0.01 M NaCl solution at a pH between 5 and 7. In particular para substituted $La(4\text{-}NO_2cin)_3$ gave the best results with 92% inhibition after the seven day immersion.

The time dependant behaviour demonstrated that these inhibitors act by suppressing the anodic reactions in the initial stages, followed by the inhibition of the cathodic processes after a longer exposure period of the steel to the inhibition solution. Electrochemical measurements based on CPP confirmed that these compounds are mixed inhibitors.

This work is consistent with previous work on Ce(salicylate)$_3$ where the mixed inhibition and synergy was attributed to the absorption of the inhibitor via the organic component in the first instance to form an iron–carboxylate bond, followed by the formation of a mixed metal Ce-Fe-carboxylate compound. This surface compound clearly affects the cathodic reaction. Following from this and based on the electrochemical behaviour reported here, it is likely that the cinnamate based compounds have a similar inhibition mechanism. The details of this will be examined via surface analysis techniques including ATR-FTIR and XPS and will be reported elsewhere.

Acknowledgements

The authors acknowledge the Australian Research Council for funding through the Special Research Centre for Green Chemistry.

References

1. W.J. Wittke, *Met. Finish.* **87** (1989) 24.
2. 'Toxicological Profile for Chromium', US Public Health Service, Syracuse, NY (1989).
3. P.T. Anatas and T.C. Williamson, 'Green Chemistry: Designing Chemistry for the Environment' (American Chemical Society, Washington DC, 1996).
4. G.D. Wilcox, D.R. Gabe and M. E. Warwick, *Corros. Rev.* **6** (1986) 327.
5. J.W. McCoy, 'Chemical Treatment of Cooling Water' (Chemical Publishing Co., New York, 1974).
6. B.R.W. Hinton, Proc. Corrosion 89, National Association of Corrosion Engineers, New Orleans, LA (1989).
7. H.S. Isaacs, A.J. Davenport and A. Shipley, *J. Electrochem. Soc.* **138** (1991) 390.
8. N.N. Greenwood and A. Earnshaw, 'Chemistry of the Elements' (Pergamon, Oxford, 1984).
9. B.P.F. Goldie and J.J. McCarroll, 'Method of Inhibiting Corrosion in Aqueous Systems', AU-32947/84, Australia (1984).
10. B.R.W. Hinton, P.N. Trathen, L. Wilson and N.E. Ryan, Proc. 28th Australasian Corrosion Association conference, Australasian Corrosion Association, Perth, Australia (1988).
11. P.K. Lai and B.R.W. Hinton, Proc. Corrosion and Prevention 95, Australasian Corrosion Association, Perth, Australia (1995).
12. A.D. Mercer, Proc. 5th European Symposium on Corrosion Inhibitors, Ferrara, Italy (1980).
13. M.H. Shawky, M.N. Moussa, F.I.M. Taha and A.S. Fouda, *Corros. Sci.* **21** (1981) 439.
14. R.D. Granata, P.C. Santiesteban and H.J. Leidheiser, Proc. The Electrochemical Society, Bethlehem, Philadelphia (1986).
15. K. Wilson, M. Forsyth, G.B. Deacon, C. Forsyth and J. Cosgriff, Proc. 9th European Symposium on Corrosion Inhibitors, Ferrara, Italy (2000).
16. K. Wilson, M. Forsyth, G.B. Deacon, C. Forsyth and J. Cosgriff, Proc. Corrosion & Prevention 2000, Australasian Corrosion Association, Auckland, New Zealand (2000).
17. S.G. Leary, G.B. Deacon, P.C. Junk, G. Myer, A.H. White, B.W. Skelton, M.H. Hilder and C. Bromant, to be published.
18. ASTM-G1-90, Standard Practice for Preparing, Cleaning and Evaluating Corrosion Test Specimens, *in* 'Annual Book of ASTM Standards', Philadelphia (1999), pp. 9–14.
19. ASTM-G31-72, Standard practice for laboratory immersion corrosion testing of metals, *in* 'Annual Book of ASTM Standards', Philadelphia (1999), pp. 107–113.
20. ASTM-G61-86, Standard test method for conducting cyclic potentiodynamic polarization measurements for localized corrosion susceptibility of iron-, nickel-, or cobalt-based alloys, *in* 'Annual Book of ASTM Standards', Philadelphia (1999), pp. 239–242.
21. B.R.W. Hinton, *J. Alloys Compd.* **180** (1992) 15.
22. R.D. Granata, P.C. Santiesteban and H.J. Leidheiser, Proc. 6th European symposium on 'Corrosion Inhibitors', Ferrara, Italy (1985).
23. M. Stern and A.L. Geary, *J. Electrochem. Soc.* **104** (1957) 56.
24. M. Forsyth, K. Wilson, T. Behrsing, C. Forsyth, G.B. Deacon and A. Phanasgaonkar, *Corrosion* **58** (2002) 953.
25. D.A. Jones, 'Principles and Prevention of Corrosion' (Prentice Hall 1996).